

Hazard Assessment of Portable Gasoline Container Flammability

A Master Thesis Submitted to the Faculty of the
WORCESTER POLYTECHNIC INSTITUTE
in partial fulfillment of the requirements for the
Degree of Master of Science in Fire Protection Engineering

Brian E. Elias

September, 2011

Approved:

Professor Ali S. Rangwala, Advisor

Professor Robert G. Zalosh, Co-Advisor

Professor Kathy A. Notarianni, Department Head

Contents

Acknowledgements

Introduction

Experimental Method

Mathematical Model

Results and Analysis

Conclusions

References

Appendices

Appendix A: Experimental Equipment Photographs

Appendix B: Computer Code for Mathematical Model

Appendix C: Photographs of PGC Ignition Testing

Acknowledgements

I would like to offer my sincere thanks and appreciation to my advisor, Professor Ali Rangwala for his unyielding support and dedication to my learning and research. His ability to analyze my work, ask the difficult questions, and keep me pointed in the right direction has made this work possible and enjoyable.

I would like to extend my thanks to Professor Robert Zalosh for his technical expertise and knowledge in every phase of this study.

Special thanks to Scott Rockwell for designing and building the environmental chamber used in the experimental study, and to my other lab mates, Kulbushan Joshi and Yanxuan Xie for their assistance with experiments and demonstrations. I also would like to thank Professor John C. MacDonald for his assistance with gas chromatography / mass spectroscopy techniques and Kelly Horiuchi from Columbia Analytical Services for her analysis of headspace grab samples.

Finally, I extend my thanks to the entire ASTM F 15.10 Subcommittee on Portable Fuel Containers – particularly Len Morrissey and Phil Monckton for funding support throughout the project.

Chapter 1

Introduction

In the United States, more than 20 million portable gasoline containers (PGC's) are sold annually, with over 46% of U.S. households having at least one [1]. Given the ubiquitous nature of the PGC, it is not surprising that studies concerning PGC safety have been in various literature reports for nearly four decades. As early as 1973, Consumer Reports demonstrated the potential for a PGC to explode as a result of flame propagation through the pour spout. More recently, Hasselbring describes a scenario where a PGC is used to pour fuel on a fire that was thought to have self-extinguished, resulting in an explosion that caused significant personal injury [2]. This type of deflagration occurs most frequently during the pouring of gasoline [3] and requires that a flammable mixture of gasoline vapors exist along the length of the pour spout and into the headspace of the PGC.

Under typical conditions involving a semi-full PGC at room temperature, the high volatility of gasoline produces headspace vapors that are too fuel rich to support flame propagation, and the risk of explosion is small. However, in conditions such as small liquid volumes, low temperatures, or certain pour angles, a flammable region can develop in this space. This type of scenario is shown in Figure 1, where a flammable vapor zone exists in the area between the liquid gasoline and the pour spout tip. The lower area close to the liquid surface is above the upper flammable limit, while the area farthest from the liquid is below the lower flammable limit. As the various controlling parameters are adjusted, the position and width of this flammable vapor zone shifts within the PGC, altering the potential for flame propagation.

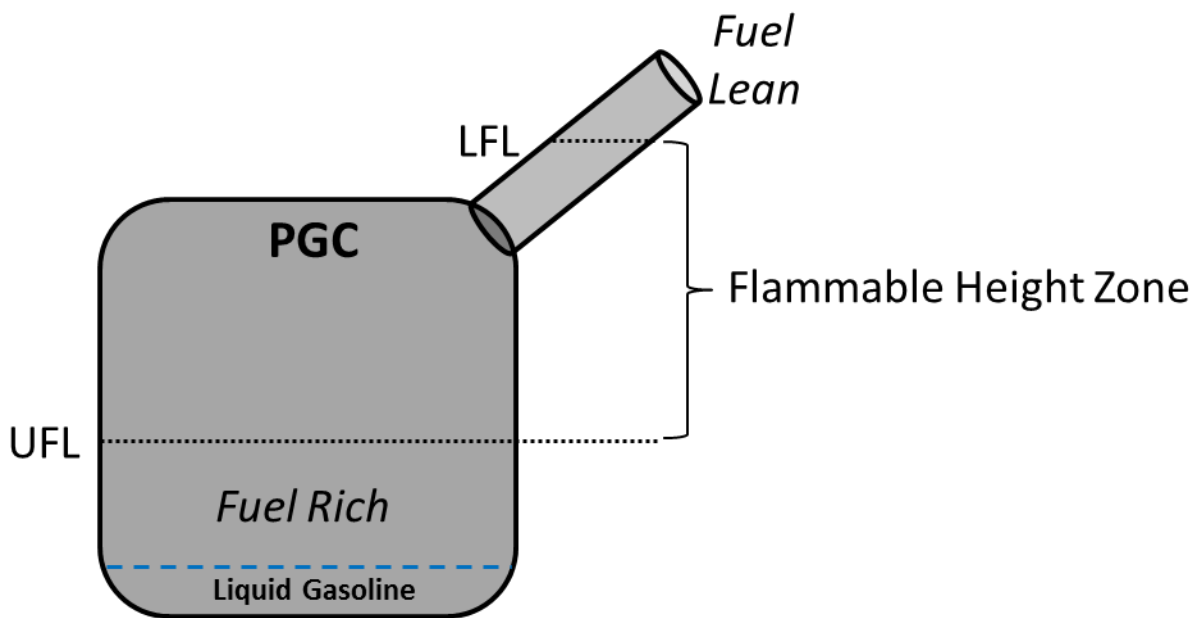


Figure 1. Flammable height zone within a PGC.

The research presented here focuses on the determining and predicting the location of this flammable band under various conditions that would be expected during consumer use of a PGC and relating these findings to an overall assessment of the flammability hazard. This task is complicated by the multi-component and dynamic nature of gasoline. Automotive gasoline may contain in excess of 200 different hydrocarbons, along with other additives, and environmental agents. An analysis by Harley provides a quantitative listing of the most abundant organic species found in the headspace of a California blend of regular gasoline; results are shown in Table 1 [4]. In addition to the multi-component nature of the headspace vapors, the liquid gasoline blend is dependent on multiple factors such as manufacturer, geographic location, time of the year, octane rating and ethanol content [5]. This variability makes it difficult to establish a single model suitable for predicting the flammable vapor location inside the relatively small confines of a PGC.

compound	wt %	vol %
isopentane ¹	24.1	27.05
n-pentane ¹	14.2	15.94
2-methylpentane ¹	9.3	8.74
ethanol	7.6	13.36
n-butane ¹	7.4	10.31
3-methylpentane ¹	5.3	4.98
2,2-dimethylbutane ¹	4.9	4.60
n-hexane ¹	4.3	4.04
2,3-dimethylbutane ¹	3.4	3.19
2,2,4-trimethylpentane ¹	2.7	1.91
methylcyclopentane	2.7	2.60
toluene	1.9	1.67
cyclopentane	1.4	1.62

Table 1. Measured weight percent of the most abundant organic species in gasoline headspace vapors of California blend fuel [4]. ¹Alkane

Previous research in the area of small vessel gasoline storage is quite limited and based on ignition testing. In this test method, a small ignition source is placed near the area of flammable vapors and a positive or negative explosion result is recorded. Gardiner, et al. use this method to evaluate the flammability of gasoline vapors in an automobile fuel tank [6]. Their work suggests a method to predict the vapor pressures of various sample of gasoline, however they do not report on the effects of a smaller container geometry or fuel pouring on the development of hazardous vapors [6]. Research conducted by Hasselbring also uses ignition based testing to provide “explosion / no-explosion” data points for various amounts of liquid fuel inside a PGC [2], however no data is published as to the fuel type, ambient temperature and other testing specifics required for repeatability. In addition, prior studies have not reported vapor-air concentration which is crucial for modeling the scenario under consideration.

The results produced by the ignition based testing method discussed above are limited to providing only positive or negative findings, making it impossible to quantify the flammability of the mixture or to quantify the influence of the various controlling parameters. Small changes to the liquid volume, temperature, pour angle, or ignition source strength may result in a different ignition outcome for seemingly similar conditions. Additionally, the absence of quantifiable flammability data makes it difficult to apply a predictive model to the result and requires iterative testing for any changes in the gasoline properties.

In contrast to ignition based testing, a new method of direct measurement of vapor concentration is used in this work and presented in Chapter 2. In this method, measurements are taken with a paramagnetic oxygen analyzer as well as an infrared (IR) sensor calibrated for n-butane. The reported concentrations are verified by laboratory analysis of select vapor samples using gas chromatography with a flame ionization detector (GC/FID). The vapor concentration data is then correlated to flammability limits and the conditions required for flame propagation within the PGC are identified in terms of the controlling parameters.

Using this test method, experiments have been conducted to quantify the flammability of the vapor space within the PGC for two different scenarios: fuel storage, and fuel pouring. The first set of test conditions is applicable to the condition where the PGC is stored in an air-tight configuration for an indefinite period of time, i.e. on a consumer's garage floor for months at a time. Experimental results identified the controlling parameters for vapor concentration as ambient temperature and the ratio of liquid fuel to PGC headspace volume. In particular, the

highest hazard is identified under conditions of small liquid volumes and low ambient temperatures – an increase in either produces a vapor that is too fuel-rich to support combustion.

The second series of tests approximates the conditions of a consumer pouring fuel from a tilted container, which may represent the most likely scenario for a PGC explosion. Specifically, in addition to a tilted container, the highest risk occurs when the liquid flow has stopped and only heavy vapors remain in the tank – i.e. the “last few drops” of fuel are poured out of the can.

This finding can be explained by examining the two common types of container pour spouts in which liquid fuel and makeup air flowing simultaneously. In the first configuration (Figure 2), two separate channels are present within the pour spout: one larger channel for outward fuel flow and one smaller channel for air inflow. In the case of fuel pouring, each channel is completely filled with either fuel or air and there is little potential to create a flammable vapor concentration inside the spout. In the second configuration – common on older can styles – only one channel exists in the pour spout for outflowing liquid and inflowing air (Figure 3). This configuration provides a long path for fuel-air mixing and results in a fuel rich air stream that is unlikely to support combustion.

In contrast to the liquid flowing scenarios described above, a scenario involving only heavy vapors flowing from the PGC allows for significantly more fuel / air mixing which may lower the vapor concentration to within the flammable range. Using this rationale, the focus of the second series of tests is on replicating the conditions immediately after the liquid has stopped pouring from the can and only fuel vapors remain.



Figure 2. Newer style PGC pour spout with two channels for separate air and liquid flow.



Figure 3. Older style PGC pour spout with a single channel for both air and liquid flow.

A data model for predicting the vapor concentration during container pouring is presented in Chapter 3. This modeling approach uses a set of mass balances, combined with familiar vent flow relations to predict the vapor concentration within the PGC and pour spout under various conditions. The overall controlling parameters are shown in Figure 4 and consist of factors

affecting the rate of evaporation and factors affecting the mixing of fuel and air vapors. These parameters are incorporated into the data model and calculations are performed using a simple fourth-order Runge Kutta algorithm, which can be easily modified to account for various can styles and changes in fuel properties.

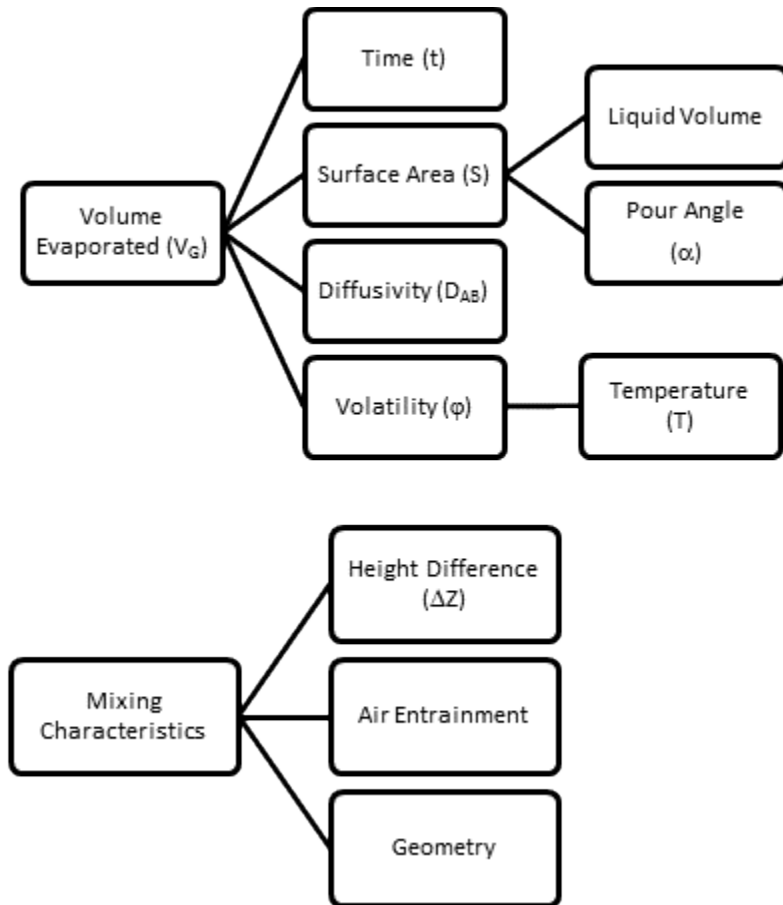


Figure 4. Factors influencing PGC headspace vapor concentration.

The results of experimental testing for both the fuel storage and fuel pouring scenarios are presented and compared with model predictions in Chapter 4. In the fuel storage tests, it was found that small gasoline volumes and/or low ambient temperatures produce conditions inside the PGC that may allow flame propagation to occur. In the fuel pouring tests, it was found that

certain combinations of liquid fuel volume, temperature and container tilt angle produced a flammable environment as well. The data model is shown to successfully predict the steady state vapor concentration found during the pour experiments.

Finally, additional information and details are provided in the appendices. Details and photographs of the experimental method and testing apparatus are provided in Appendix A; Appendix B contains the computer code for the mathematical model (Polymath); and Appendix C contains photographs of PGC ignition testing used to validate our vapor concentration measurements.

Chapter 2

Experimental Method

2.1 Experimental Apparatus

Experiments were conducted using a commercially available plastic 19 liter (5-gallon) PGC with a child resistant, auto-close pour spout. The spout is 2.54 cm in diameter with an inner channel for liquid flow and a second, smaller channel for make-up air to enter the can (see Figure 5). In order to facilitate passage of the sample acquisition tubing, a 6.35 mm hole was drilled approximately 1 mm below the pour spout base as shown in Figure 5. In the first series of tests for gasoline storage scenarios, the automatic closing spout was not modified and left in the fully closed position; the PGC was considered airtight for these tests. In the second series of tests for the fuel pouring scenario, the spring-loaded automatic closure mechanism was disabled and the pour spout was secured in a fully open configuration in order to allow for free vapor flow. Fuel pouring tests were conducted at a constant temperature of 20°C and the PGC was mounted to a tilt-apparatus allowing for pour angles (α) between 61° and 73° with the vertical. Aside from the spout modification, the PGC used in both test series was identical.

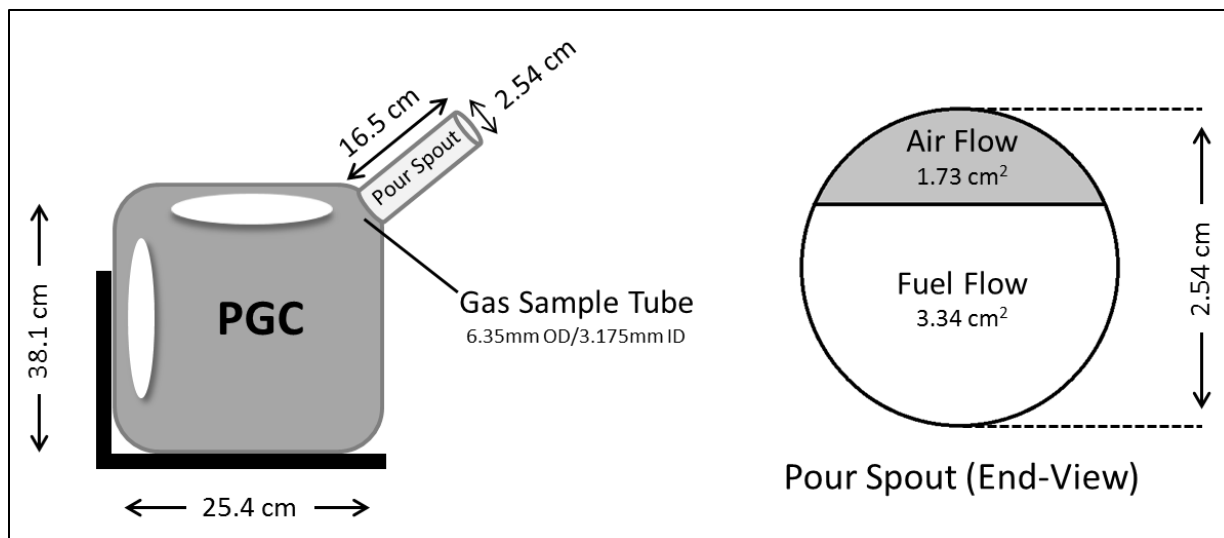


Figure 5. Portable gasoline container dimensions and sampling location for static testing.

In both test series, vapor sampling was performed by introducing a length of sample tubing into the PGC at the desired location. In the static storage tests, sampling was conducted at the base of the pour spout as shown previously. In the fuel pouring tests, in addition to the base, sampling was also conducted at the outside tip of the pour spout exit. The sampling line used is Teflon tubing with an inner diameter of 3.175 mm and an outer diameter of 6.35 mm; fittings are compression-style manufactured by Swagelok. A vapor pump rated for combustible vapors is used to supply the instrumentation with a constant flow rate of 0.25 liters per minute of sample gas.

Experimental tests were performed inside a custom-designed environmental chamber with dimension of 1.2 m x 0.86 m x 1.1 m. The chamber is capable of maintaining temperatures as low as -25 °C for a duration of 2 hours. Cooling is provided by dry ice loaded into 6 copper tubes on the enclosure walls; tubes have a diameter of 54 mm and a height of 1.0 m. Air circulation is provided by a fan blade inside the chamber. The fan motor is mounted external to

the chamber to ensure a spark-free environment for testing. An evenly spaced thermocouple tree consisting of 8 type-K thermocouples is mounted inside the chamber near the PGC and runs the full vertical height of the chamber. With the fan switched on, it was possible to achieve a consistent top-bottom temperature profile to within ± 2.5 °C. The temperature profile is recorded throughout the test duration by a PC-based data acquisition system supplied by Measurement Computing Corporation. Photographs of the chamber are shown in Appendix A.

Vapor concentration measurements for the static storage tests were made using an infrared (IR) sensor calibrated for n-butane. The device is a factory modified Altair-5 manufactured by Mine Safety Appliances and has a published accuracy of ± 1.0 vol% butane. The factory modification involved disabling the internal vapor pump, allowing for the use of the external combustible-vapor rated pump. An IR sensor was selected over a catalytic bead sensor because of its resistance to poisoning at high vapor concentrations, and its ability to measure concentrations above the upper flammable limit. The IR sensor also has the advantage of being sensitive to multiple hydrocarbons with similar absorptivity characteristics to the calibrated compound. In the case of gasoline, many of the volatiles are C₄ and C₅ based hydrocarbons with similar C-H bonds having a similar IR absorption band.

Measurements for the fuel pouring tests were conducted with a Servomex Servotough paramagnetic oxygen analyzer connected in series with the infrared sensor. This device has a published resolution of ± 0.05 vol% oxygen and was configured by the manufacturer to allow for the use of solvent-based vapors. This modification consisted of fitting the unit with stainless steel tubing and PTFE seals. The configuration selected meets U.S. Coast Guard requirements

for oxygen analysis in gasoline vent lines during ship-to-dock fuel transfer. The addition of the oxygen analyzer provided a second instrument for vapor analysis and verification of the test measurements obtained from the infrared sensor. Vapor concentration readings from both instruments were recorded and compared for consistency at the conclusion of each test.

As a final verification of instrument accuracy, grab samples were collected by connecting a Summa canister in-line with the vapor sample line. These canisters were vacuum purged and backfilled with nitrogen such that opening the canister valve allowed 0.25 liters of sample gas to enter the canister. Samples were obtained at various concentration readings and sent for laboratory analysis to confirm the accuracy of both the infrared sensor and the oxygen analyzer.

2.2 Experimental Procedure

The gasoline used for this study was obtained at a gasoline filling station located in Worcester, MA (USA) in October, 2009 and stored in a plastic PGC with an o-ring seal on the closure cap. The gasoline is regular blend and is indicated as containing 10% ethanol by volume and the Reid Vapor Pressure is estimated at 90 kPa [5]. The unused portion of the fuel sample was analyzed at the conclusion of experimental testing and found to have a Dry Vapor Pressure Equivalent of 86.3 kPa, indicating a drop in vapor pressure of 4.1% due to fuel weathering.

The static fuel storage tests were conducted inside the environmental chamber after the temperature had stabilized. At this time, the desired quantity of liquid gasoline was withdrawn from the storage container and placed in an airtight glass bottle inside the environmental chamber for a period of 30 minutes to allow for temperature equalization. The gasoline is then

measured and transferred into the PGC, the pour spout is reattached, and the gasoline is permitted to evaporate inside the PGC for 5 minutes.

At the end of the 5 minute evaporation time, the sampling pump is switched on and readings are obtained from both the oxygen analyzer and the IR sensor. Values are recorded when a stable reading ($\pm 0.1\%$ oxygen) is present for 10 seconds. The sampling pump is permitted to run for a maximum of 30 seconds per test in order to avoid significantly reducing the pressure in the PGC. If a stable reading is not obtained at the end of the 30-second period, a new trial with fresh gasoline is performed. The PGC is evacuated of any residual vapors between experimental runs by flushing with compressed air for a period of 15 minutes. Successful flushing is confirmed by instrument readings showing no gasoline vapor present in the PGC.

Experimental testing for fuel pouring scenarios is conducted in a similar manner. In these tests, liquid fuel at 20°C is measured and poured into the PGC. The PGC is set to the desired pour angle and sample measurement begins immediately. Over the range of liquid volumes and pour angles tested, no combination resulted in liquid fuel entering the pour spout or vapor sampling port – only gasoline vapors were permitted to flow through the pour spout during testing. In addition, since the pour spout is fixed in an open configuration there is no concern with depressurizing the PGC over longer sample acquisition times. The sampling is permitted to continue until a stable reading ($\pm 0.1\%$ oxygen) is present for 30 seconds.

Chapter 3

Mathematical Model

The mathematical model presented here is developed to calculate the time-dependent concentration of fuel vapor within the PGC during the simulated pouring tests. Specifically, it is desired to model how the fuel vapor concentration changes in the time immediately following the container being tilted – i.e. the hazardous “last few drops” scenario.

In comparison to previous models available for the evaporation of gasoline, the model presented in this work is applicable to the small liquid and headspace volumes found within a PGC. In addition, the container tilt angle during pouring is found to have a significant role in determining the vapor concentration and is considered in this model. The influence of this tilt angle, α , is shown in Figure 6, which depicts a PGC undergoing a progressive tilt, as would occur during consumer pouring. Beginning with the container in a flat position (i.e. a tilt angle of zero degrees), any increase in angle causes an increase in the height of the vapor column, ΔZ . This causes an increase in the flow of both outgoing fuel vapor and incoming air. The overall effect is a widening of the flammable vapor zone as the fuel-rich headspace vapor mixes with ambient air.

The second parameter influenced by the container tilt angle is the liquid surface area available for evaporation. At shallow angles up to 45 degrees, shown on the first row of Figure 6, an increase in the container tilt angle causes a decrease in the liquid surface area as the liquid begins to assume a wedge-shaped configuration. This results in a lower rate of evaporation which, in addition to the increasing ΔZ discussed above, acts to widen the flammable vapor zone by decreasing the concentration of fuel vapors.

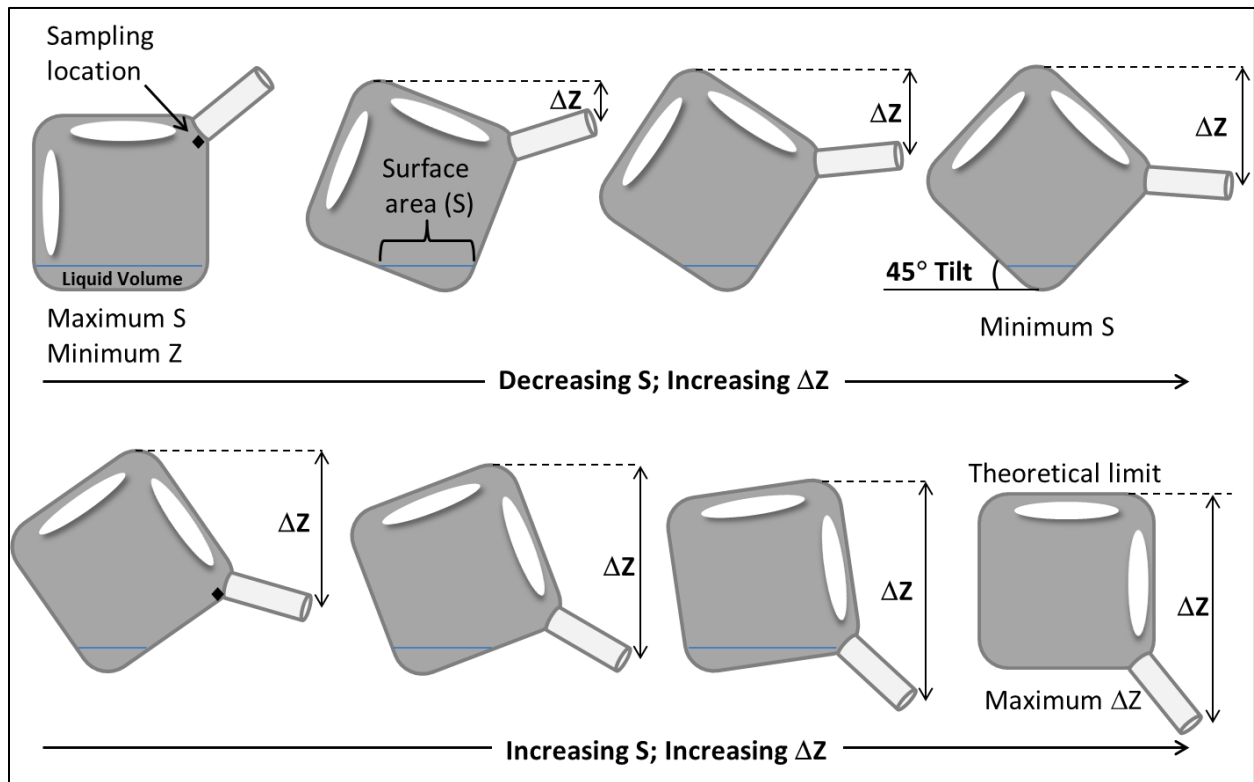


Figure 6. Influence of pour angle on surface area (S) and mixing height (ΔZ).

The cases of steeper pour angles represent the scenario of a consumer pouring the “last few drops” of gasoline from a nearly empty container, and are of significant importance in quantifying the flammability hazard. At these angles, shown in the lower row of Figure 6, a further increase in the angle causes the opposite effect of increasing the liquid surface area for evaporation. At the same time, the increasing angle also causes an increase in the fuel-air mixing due to the increasing ΔZ value. These two effects work in opposition and the influence on the flammable vapor zone is dependent on their comparative magnitudes.

3.1 Overall Mass Balance

The scenario is modeled by considering the PGC headspace and pour spout as a single well-mixed volume as shown in Figure 7. The total mass within the system, \dot{M}_{total} is then a function of: 1) the inflow of ambient air, \dot{M}_{in} , 2) the outflow of the headspace vapors, \dot{M}_{out} , and 3) the rate of evaporation of gasoline, \dot{M}_{evap} . The overall mass balance for the system is given by:

$$\frac{dM_{total}}{dt} = \dot{M}_{in} - \dot{M}_{out} + \dot{M}_{evap} \quad (1)$$

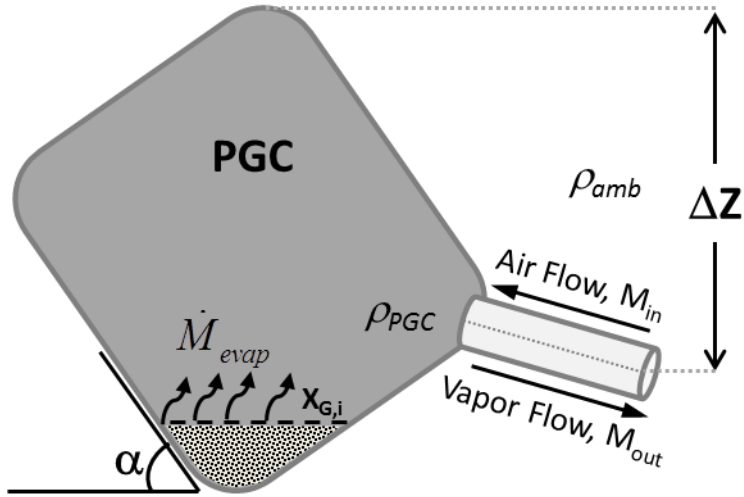


Figure 7. Parameters for PGC vapor concentration model.

3.2 Mass Inflow and Outflow

The vapor-air mixture inside the PGC comprises of heavy gases as shown in Table 1 resulting in a density gradient across the pour spout. This gradient serves as the driving force for mass transport of air (coming in) and heavy vapor (going out) across the pour spout. The pressure difference across the spout opening, ΔP , can be calculated as a function of the height of the headspace volume, ΔZ , from the following hydrostatic equation:

$$\Delta P = P_{PGC} - P_{amb} = g \int_0^Z (\rho_{PGC} - \rho_{amb}) dZ \quad (2)$$

where: P_{PGC} is the pressure within the PGC at the level of the pour spout exit,
 P_{amb} is the ambient pressure at the level of the pour spout exit,
 ρ_{PGC} is the density of the headspace vapor mixture inside the PGC,
 ρ_{amb} is the density of the ambient air,
 Z is the height above the pour spout exit as shown in Figure 4 and
 g is the acceleration of gravity.

If it is assumed that the densities of the headspace vapor is uniform (i.e. a well-mixed approximation), then Equation 2 simplifies to

$$\Delta P = P_{PGC} - P_{amb} = (\rho_{PGC} - \rho_{amb}) \Delta Z \quad (3)$$

The mass flow through the spout can then be expressed as

$$\dot{M}_{out} = \rho_{PGC} A \sqrt{\frac{2g(\rho_{PGC} - \rho_{amb}) \Delta Z}{\rho_{PGC}}} \quad (4)$$

where: A is the cross sectional area of the pour spout tube.

As the buoyant flow outward continues, the pressure within the PGC will fall slightly below atmospheric causing ambient air to enter the can through the pour spout tube. In order to determine the rate of air inflow, the container volume is assumed to remain fixed such that the volume of inflowing air must be equal to the volume of exiting headspace vapor. Expressed in terms of mass flow rates, this relation becomes

$$\dot{M}_{in} = \dot{M}_{out} \frac{\rho_{amb}}{\rho_{mix}} \frac{A_{in}}{A_{out}} \quad (5)$$

where: $\frac{A_{in}}{A_{out}}$ is the ratio of inflow area to outflow area.

3.3 Evaporation Rate

The rate of evaporation of liquid fuel is dependent on the vapor pressure of the gasoline (P_{vap}), the diffusivity of the gasoline vapors in air (D_{AB}), and the liquid surface area available for evaporation (S). A modified version of Fick's second law incorporates these parameters and is used to calculate the rate of evaporation of the liquid fuel. This modified form, as presented by Arnold [7], adds a correction term, ϕ , to Fick's second law to account for deviations due to the high mass transfers rate associated with hydrocarbon fuels. The Arnold model for the rate of evaporation is expressed as

$$\dot{M}_{evap} = S\phi\sqrt{\frac{D_{AB}}{t}}(\rho_G) \quad (6)$$

where: ρ_G is the density of gasoline vapor.

Using the relation suggested by Arnold, the value of the volatility correction term, φ , is calculated as a function of the interfacial gas concentration, X_{Gi} . The resulting equation is

$$\varphi = \frac{1}{\sqrt{\pi}} \frac{X_{Gi}}{1 - X_{Gi}} \frac{\exp(-\varphi^2)}{1 + \operatorname{erf}(\varphi)} \quad (7)$$

The interfacial gas concentration is calculated on the assumption that an interfacial equilibrium is established and that the mixture formed can be considered ideal. Using these assumptions, the value of X_{Gi} is the vapor pressure of gasoline, P_{vap} , divided by the ambient pressure, P_{amb} . The vapor pressure used is 45 kPa, as reported by Okamoto et al. for a similar blend of un-weathered gasoline at 20 °C [8].

3.4 Alternate Method to Calculate Evaporation Rate

In the Arnold model it is assumed that liquid evaporation occurs into a volume of infinite height, such that the concentration at the highest point is equal to zero. This assumption is a reasonable approximation for the most hazardous PGC scenarios involving low temperatures and low liquid volumes. In these cases, the partial pressure of gasoline vapor in the headspace is only a small fraction of the saturation vapor pressure at the liquid surface. The driving force for evaporation remains approximately equal to that given by the Arnold model.

However, in situations involving higher temperatures or larger liquid volumes, the difference in the partial pressure of gasoline vapor between the liquid surface and the headspace is lower,

resulting in a decrease in the rate of evaporation. In order to account for this influence, the rate of evaporation can be calculated as a function of the difference in partial pressure. The equation is then of the form suggested by Matthiessen [9]:

$$\dot{m}_{evap} = \frac{(MW)kS(P_{sat} - P_G)}{RT_L} \quad (8)$$

where: (MW) is the molecular weight of gasoline,

k is the mass transfer coefficient,

P_{sat} is the saturation vapor pressure of gasoline,

P_G is the partial pressure of gasoline vapor in the headspace,

R is the universal gas constant, and

T_L is the temperature of the liquid gasoline.

In the case of gasoline, a multi-component model may offer a better fit to experimental data.

The multi-component form of Equation X is [10]:

$$\dot{m}_{evap} = \frac{kM_T^\circ \sum x_i^\circ (MW)_i (P_{sat,i} - P_G)}{RT_L n_T \sum x_i^\circ (MW)_i} \exp(-kP_{sat,i}t) \quad (9)$$

where: M_T° is the initial mass of the liquid gasoline,

x_i° is initial mole fraction of component i in the liquid,

$(MW)_i$ is the molecular weight of component i ,

$P_{sat,i}$ is the saturation vapor pressure of component i , and

n_T is the number of moles of liquid gasoline.

3.5 Species Balance

In this model, the headspace vapor above the liquid fuel is considered as a mixture of air and hydrocarbon-based gasoline vapors. This leads to a three component model of the headspace consisting of oxygen, nitrogen, and gasoline-vapor with a fixed ratio between the oxygen and nitrogen concentration of 23 mass-percent and 77 mass-percent, respectively. The species balance for the gasoline vapors is given by,

$$\frac{dM_G}{dt} = \dot{M}_{evap} - Y_G \dot{M}_{out} , \quad (10)$$

where: M_G is the mass of gasoline vapors, and

$$Y_G \text{ is the mass fraction of gasoline vapors } \left(\frac{M_G}{M_{total}} \right).$$

Oxygen and nitrogen enter the PGC from the ambient air and leave in the outflowing headspace vapor mixture. The balance for each of these species is

$$\frac{dM_{O_2}}{dt} = 0.23\dot{M}_{in} - Y_{O_2}\dot{M}_{out} \quad \text{and} \quad (11)$$

$$\frac{dM_{N_2}}{dt} = 0.77\dot{M}_{in} - Y_{N_2}\dot{M}_{out} \quad (12)$$

where: M_{O_2} is the mass of oxygen,

Y_{O_2} is the mass fraction of oxygen vapors,

M_{N_2} is the mass of oxygen, and

Y_{N_2} is the mass fraction of oxygen vapors.

3.6 Solution Strategy

The governing equations for the mathematical model consist of equations 1, 3, 4 and 5 along with the species balances shown in equations 10, 11, and 12. These equations are solved simultaneously using the Runge-Kutta-Fehlberg algorithm as implemented in the Polymath software code presented in Appendix B.

Chapter 4

Results and Analysis

4.1 Data Conversion to Total Gasoline Vapor Concentration

Experimental vapor concentration measurements are obtained using three independent techniques: infrared sensor, a paramagnetic oxygen analyzer, and a through laboratory analysis of grab samples. In order to report a final value of total gasoline vapor concentration, various conversion methods are used. In the case of the infrared sensor, the raw data is collected as a volume percent of butane present in the sample gas. The conversion from butane concentration to total gasoline vapor concentration is accomplished by using an assumed headspace vapor composition for a similar gasoline blend as provided by Harley in Table 1. From this data, it is noted that the 9 of the 13 most abundant species in the headspace vapors are basic alkanes, sharing the same infrared absorption band of $3000 - 2850 \text{ cm}^{-1}$ [11]. Using this reasoning, it is assumed that the infrared reading calibrated for n-butane is representative of all basic alkanes in the mixture (9 of the top 13 compounds). The ethanol and the aromatic compounds have significantly different infrared absorption bands of $3550 - 3200 \text{ cm}^{-1}$ and $1600 - 1450 \text{ cm}^{-1}$, respectively [11] and these are not expected to be reported by the infrared sensor. In order to account for the contribution of these species, the total gasoline vapor volume fraction ($X_{fuel \text{ vapor}}$) is calculated as:

$$X_{fuel\ vapor} = X_{IR} \left(\frac{100}{\sum X_{alkane}} \right),$$

where X_{IR} is the volume percent of butane reported by the infrared analyzer and X_{alkane} is the volume percent of each alkane present in the headspace vapor as reported in Table 1.

Instrument readings from the oxygen analyzer are recorded as volume percent oxygen present in the sample. Conversion to total gasoline vapor concentration is straightforward, and based on the assumption that the headspace consists only of air and gasoline vapor. The influence of water vapor is not incorporated in these calculations since the relative humidity in the laboratory environment is typically below 30%, due to either the outside climate or the use of air conditioning equipment. Subsequent analysis using psychrometric data for 30% relative humidity shows that the reported values would have a maximum error of -0.45 to -0.65 vol% if this were incorporated; lower concentration values would have the largest error. Using the dry air assumption, the concentration of gasoline vapor is calculated directly from the oxygen / nitrogen molar ratio.

Laboratory analysis of various grab samples of headspace vapor is used as a final verification of the accuracy of both the IR sensor and the oxygen analyzer. Laboratory results are reported as a measure of total hydrocarbons present in the headspace vapor using a modified EPA TO-3 test method, and are compared directly to the readings from the IR sensor. The correction method described above is used to facilitate comparison of the total hydrocarbons to the calculated gasoline vapor concentration as reported by the oxygen analyzer. Using this method, values for

all three analysis techniques can be compared for consistency. The maximum data spread between these three methods of measure was found to be ± 2.9 vol%, with the largest data spreads being noticed at high vapor concentrations. This may be due to the calibration of the IR analyzer, which is valid up to a maximum of 25 vol% vapor concentration. There was no evidence that one test method resulted in universally higher or lower values than another test method, indicating a small amount of random noise in all methods.

4.2 Limits of Flammability

The risk of flame propagation through the PGC pour spout is determined by the size and location of the flammability zone – the area within the PGC that contains a combustible mixture of gasoline vapors between the flammability limits. The nominal values for the lower and upper flammability limits are considered as 1.4 and 7.6 vol %, respectively, as reported for automotive gasoline [12]. Zabetakis published similar results for Grade 100/130 aviation gasoline, finding flammability limits of 1.3 and 7.1 vol % [13]. Data published by Davletshina and Cheremisinoff for automotive gasoline is also in agreement with flammability limits of 1.4 to 7.4 vol% [14]. A degree of uncertainty exists in these published values and is largely a result of the dependence of volume-percent based flammability limits on the molecular weight of the combustible vapor [13], and therefore on the fuel composition. In order to account for this uncertainty, flammability limits are expressed here as bands with an approximate bandwidth of 0.5 vol %. Using this analysis, any data point that falls between the lower edge of the lower flammable band and the upper edge of the upper flammable band is considered combustible.

4.3 Storage Configuration

Static fuel storage tests were conducted to evaluate the gasoline vapor concentration in the headspace of a PGC at various temperatures and various quantities of liquid gasoline (Figure 8). In this set of experiments, the temperature was varied from -25°C to $+20^{\circ}\text{C}$ and the volume of liquid gasoline was varied from 15 mL to 1000 mL. These data show a strong dependence of vapor concentration on both temperature and liquid gasoline volume. The dependence on liquid volume is particularly evident at small volumes. At a temperature of -10°C , the change from 15 mL of fuel to 30 mL of fuel resulted in the vapor concentration increasing from 1.2 vol % to 5.2 vol % (2.7 vol % per mL of fuel). At larger volumes the change is less pronounced. A change from 500 mL of fuel to 1000 mL of fuel resulted in the butane vapor concentration increasing from 14.7 vol % to 15.7 vol % (+0.002 vol % per mL of fuel). This is likely explained by the dependence of the fuel evaporation rate on exposed surface area. Once the entire bottom of the PGC is covered with a thin layer of gasoline, further additions of gasoline will result in increased liquid depth, however no additional exposed surface area. The overall results show that low gasoline volumes and/or low temperatures are required to produce a flammable environment within the PGC.

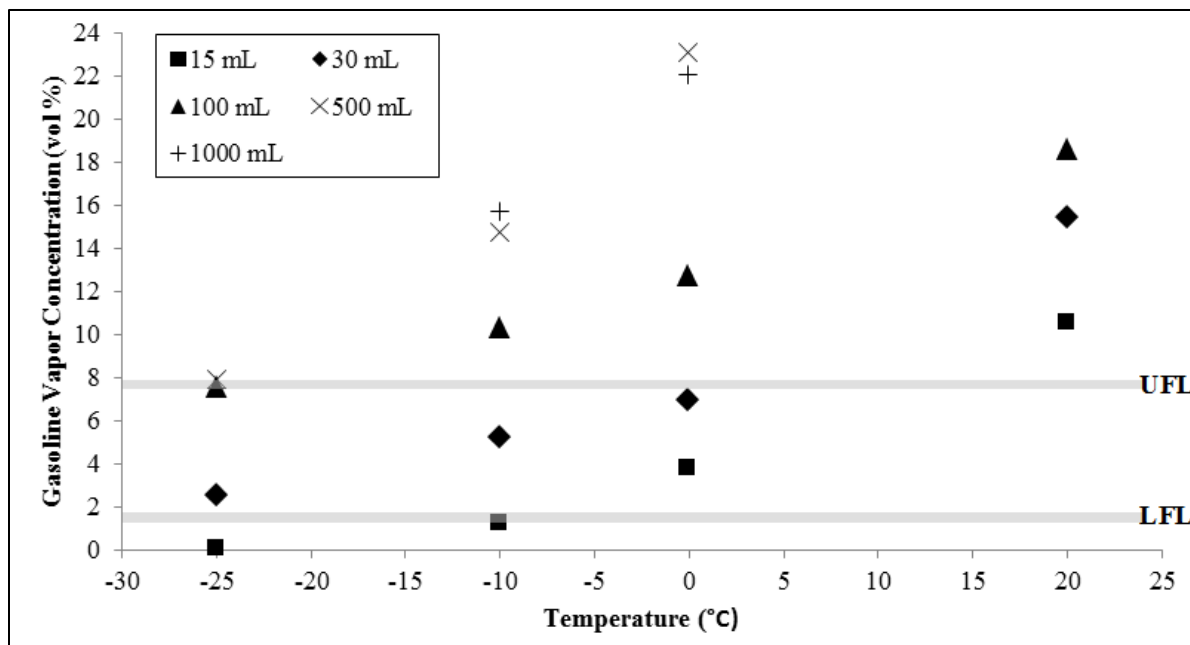


Figure 8. Influence of temperature and gasoline liquid volume on vapor concentration.

Limited volume-temperature-concentration data is available in the literature for comparison; however concentration values match anecdotal reports of the conditions required for flammability. In one case Gardiner et al., reports that a gasoline container filled 5% with liquid gasoline (946 mL in a 19-L container) is not ignitable at temperatures above 10 °C, and produces a small deflagration at temperatures below -10 °C [6]. At temperatures below -25 °C, however, the same conditions result in a rapid deflagration. Using this data, it is postulated that at approximately -25 °C, the mixture is close to the upper range of the flammability limits – near 7.6 vol% [12]. This is in reasonable agreement with the data presented in Figure 8, where 1000 mL of gasoline produced a measured total vapor concentration of 7.4 vol%.

4.4 Pouring Configuration

Fuel pouring tests have been conducted to evaluate the influence of container tilt angle on the location of the flammable vapor zone within the PGC. This evaluation requires measuring the vapor concentration at two locations: the inner pour spout base and the outer pour spout tip. These two values are used to locate the flammable vapor zone and identify the potential for flame propagation into the container.

The results of these tests are shown in Figure 9 a plot of tilt angle and liquid volume versus vapor concentration. The minimum pour angle tested is 61 degrees – at this value, gasoline vapor concentrations at the tip were below measurable quantities for all fuel volumes tested. The maximum test angle of 73 degrees represents the maximum ergonomic angle at which a consumer might reasonably tilt the can while pouring the contents.

At a liquid volume of 10 mL, concentrations at the pour spout base enter the flammable range at a tilt angle of 61 degrees. This same fuel quantity, however, does not produce any measurable fuel vapor at the spout tip regardless of tilt angle – it is not expected that flame propagation would occur at this liquid volume. Increasing the liquid volume to 30 mL increases the fuel concentration at the pour spout tip to measurable quantities; at larger pour angles the concentration exceeds the LFL at the pour spout tip. Fuel concentrations at the spout base also increase significantly, however the concentration remains below the UFL until the maximum angle of 73 degrees is tested. This resulted in two pour angles that produced flammable conditions at both the pour spout tip and pour spout base with 30 mL of liquid fuel: 69 and 71

degrees. Under these conditions, an external flame could conceivably propagate through the spout and into the PGC. Finally, increasing the liquid volume to 50 mL produces a flammable condition at the pour spout tip for the three steepest angles (69, 71 and 73 degrees), however the concentration inside the PGC is too fuel rich to support combustion. In this case of the 50 mL liquid volume, an external ignition source may result in a limited flame at the spout tip, however propagation into the container is unlikely.

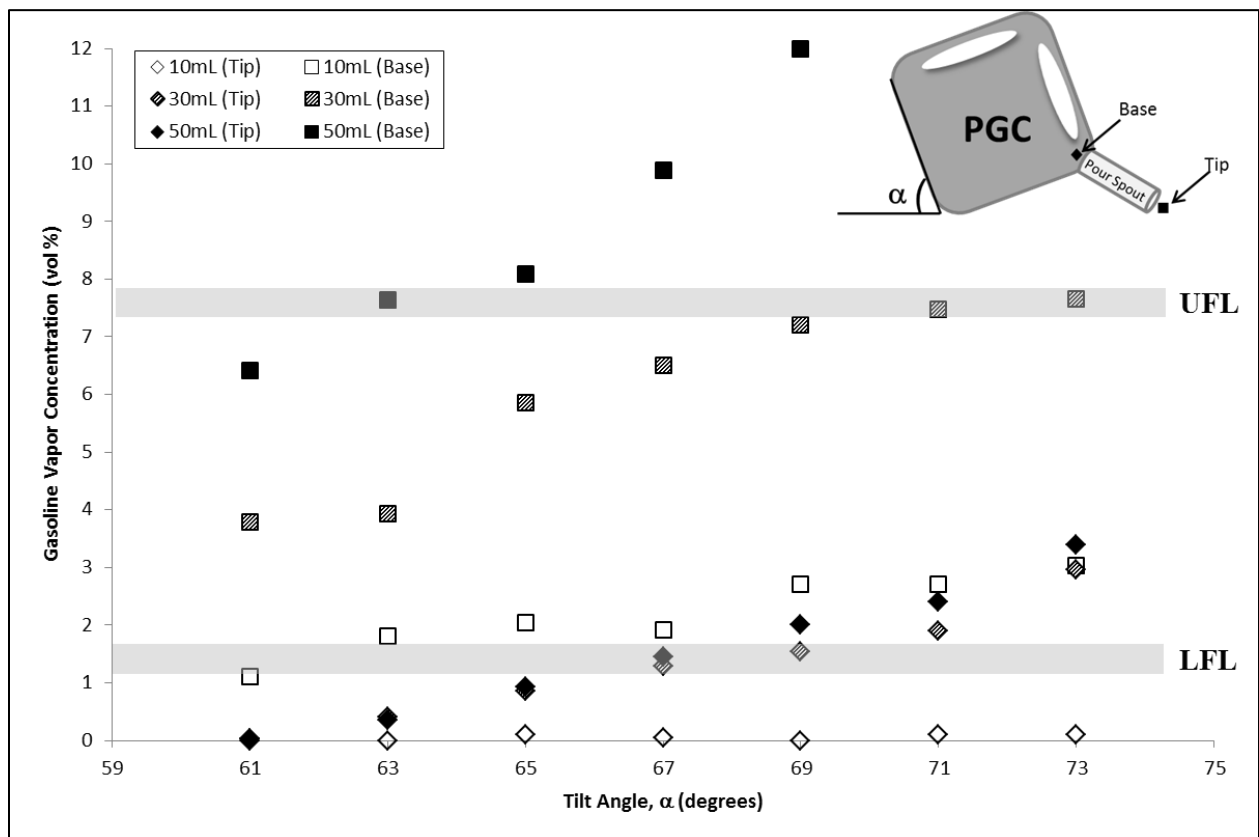


Figure 9. Influence of gasoline volume and tilt angle on vapor concentration at 20 C.

The results show that increasing the pour angle increases the vapor concentration at both the base and the tip of the pour spout. It is also noted that considerably larger fuel volumes are required to produce explosive conditions in the PGC as compared to the static fuel storage tests (Figure

8). For example in a static test at 20°C, a fuel volume of 15 mL results in a vapor concentration of 10.5 vol%, while a fuel volume of 30 mL produces vapor concentrations as low as 3.8 vol% in the pour test (Figure 8). This result is likely due to two factors: 1) The fuel surface area is smaller for a given volume when the PGC is tilted, and 2) the closed spout configuration of the static tests allows the volatiles to collect within the PGC. Both of these are expected to produce a higher vapor concentration for a given fuel volume in the static tests versus the pouring tests.

4.4 Model Validation

The purpose of the data model is to predict the movement of the flammable vapor zone within the PGC as a function of time and the variables considered previously: temperature, liquid volume, and container tilt angle. The model results are compared against data obtained from the fuel pouring experiments in Figures 10, 13, 14, and 15.

Experimental results and model predictions for a container tilt angle of 61-degrees are shown in Figure 10. The model closely predicts the vapor concentration for the case of 30 mL and 50 mL, however tends to under-predict the values at the lowest liquid level of 10 mL. This may be due to inaccuracies of the experimental data at very low vapor concentrations. At all fuel volumes, the data model follows the trend of an initially high vapor concentration and the eventual decay to near steady-state condition. The initially high values are due to the established vapor equilibrium prior to testing, and the eventual flattening of the curve occurs as the rate of fuel vapor outflow decreases and approaches the rate of evaporation from the liquid surface.

The data model also allows for prediction of the flammable vapor zone in the initial one minute time interval, during which experimental data is unreliable. In the case of 10 mL of liquid fuel with a container tilt angle of 61 degrees (Figure 10), the model calculations suggest that the vapor concentration is too fuel rich to support combustion until a time of 0.45 minutes as shown by the vertical dashed line. This is particularly useful data when determining the flammability hazard in the time immediately following liquid fuel flow – the “last few drops” scenario.

The predicted oxygen and nitrogen concentrations for the same scenario of a 61-degree tilt angle are presented in Figures 12 and 13 respectively. No direct test data is available for comparison, however each follows the expected trend for an assumed headspace composition of only air and fuel vapor.

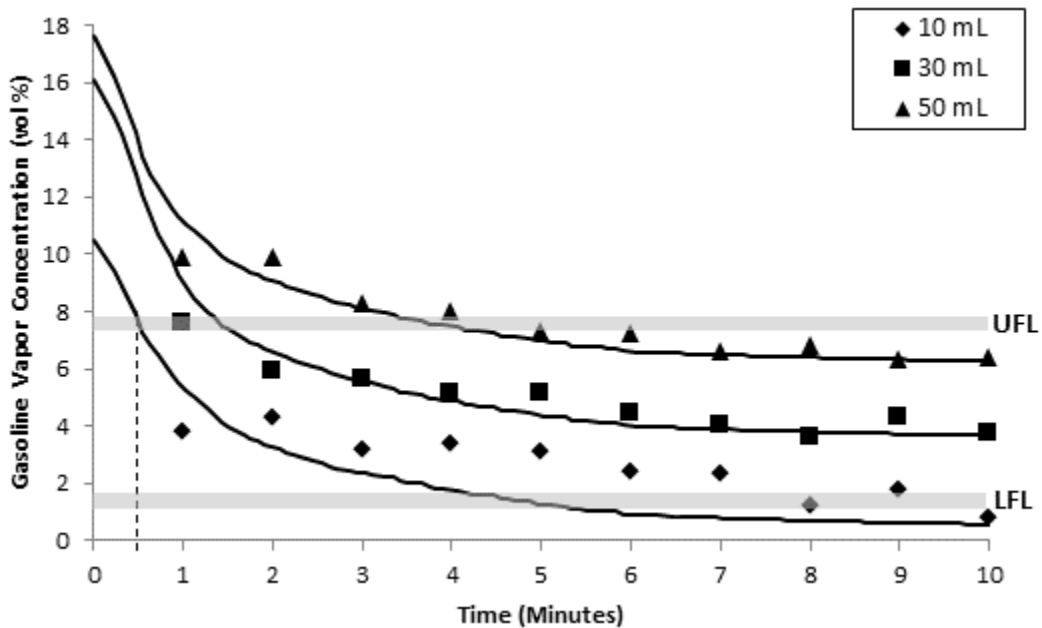


Figure 10. Comparison of experimental data to model predictions for $\alpha = 61^\circ$; dashed line indicates time to flammable vapor concentration for the 10 mL case.

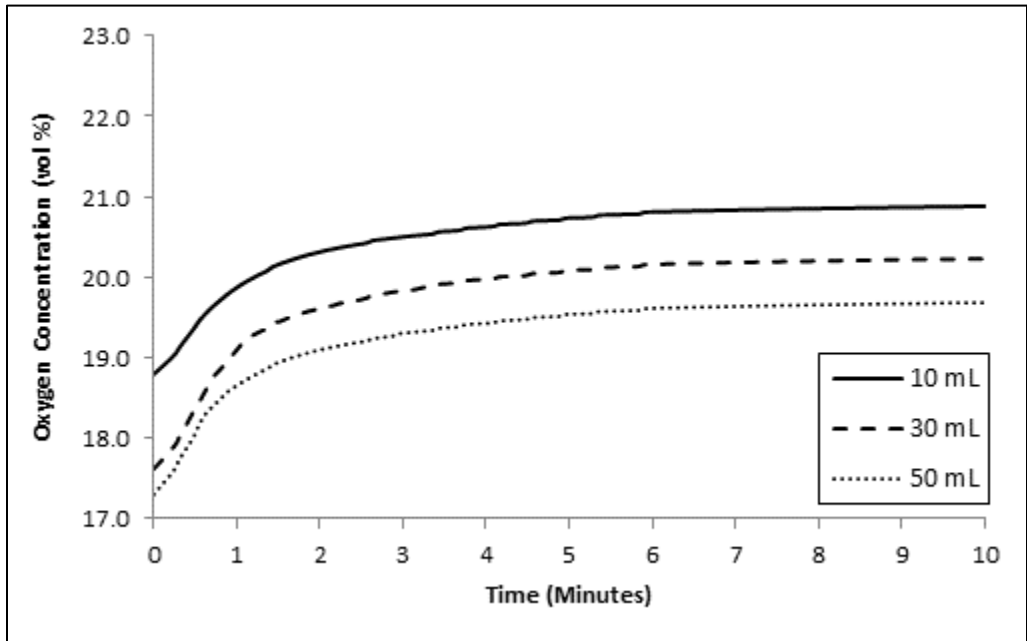


Figure 11. Oxygen concentration model predictions for $\alpha = 61^\circ$.

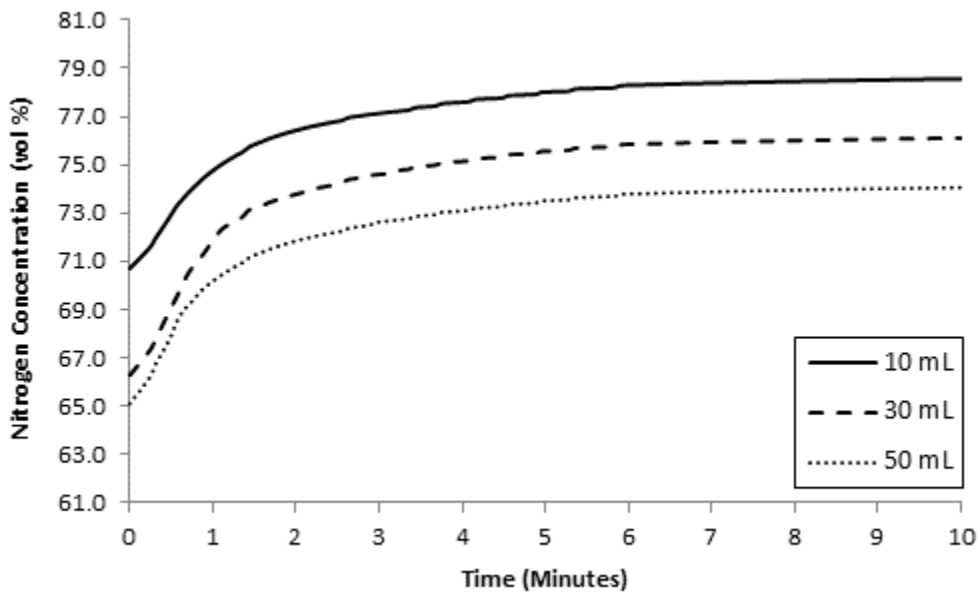


Figure 12. Nitrogen concentration model predictions for $\alpha = 61^\circ$.

Results from increasing tilt angles are presented in Figure 13 through 15. As the pour angle increases, the height difference from the top of the PGC to the pour spout (ΔZ in Figure 4) increases which leads to larger vapor and air flow rates through the pour spout. This larger flow rate results in a steeper slope of the concentration-time curves as the pour angle increases. In addition to the increase in flow rate, the larger tilt angles also result in a larger liquid surface area available for evaporation. This effect results in an upward and leftward shift of the steady-state region of the curve as the pour angle is increased.

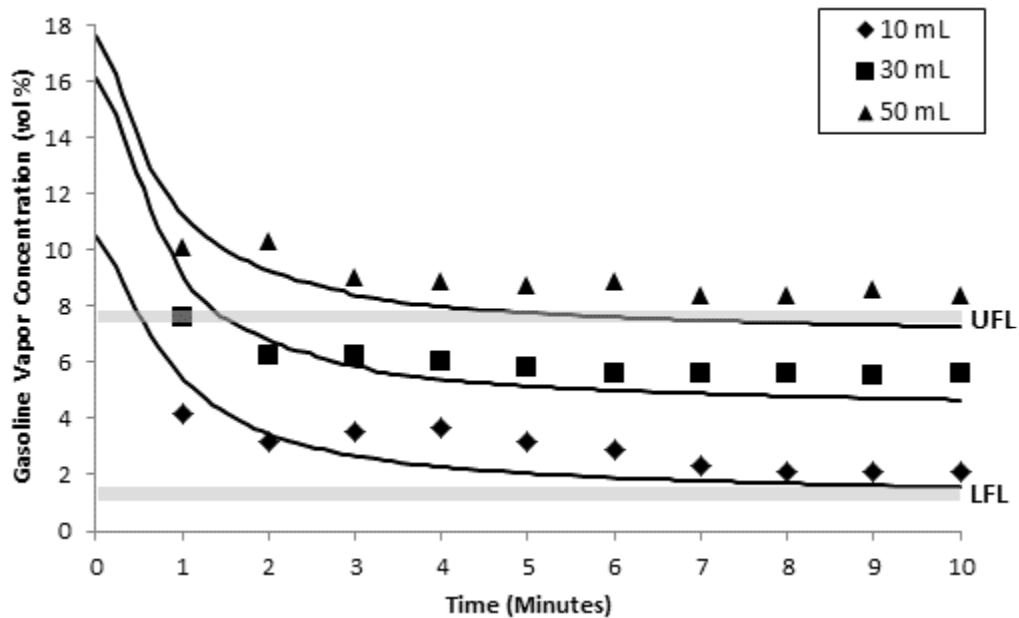


Figure 13. Comparison of experimental data to model predictions for $\alpha = 65^\circ$.

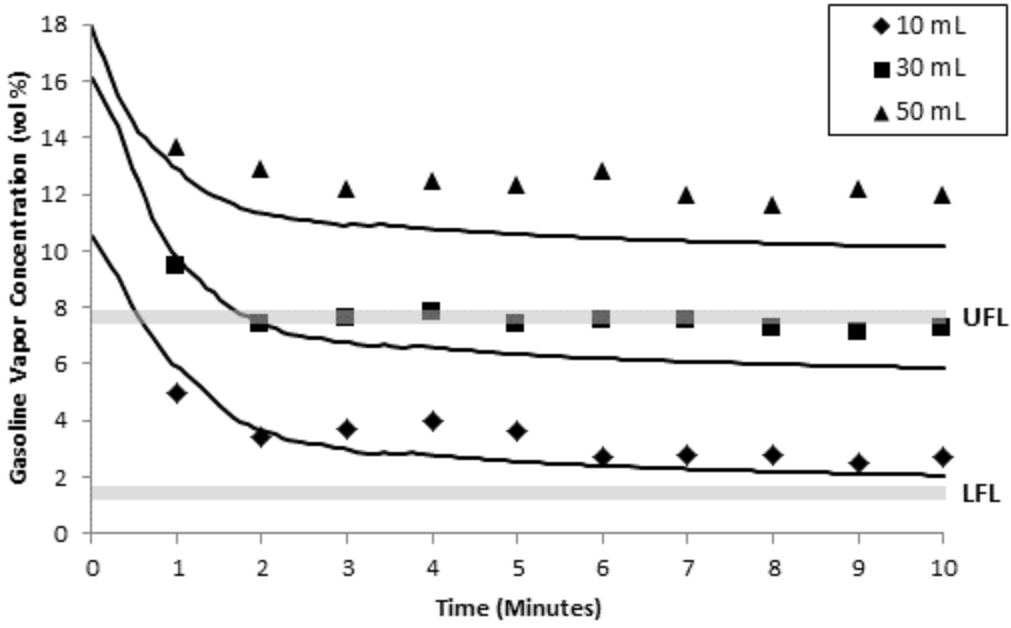


Figure 14. Comparison of experimental data to model predictions for $\alpha = 69^\circ$.

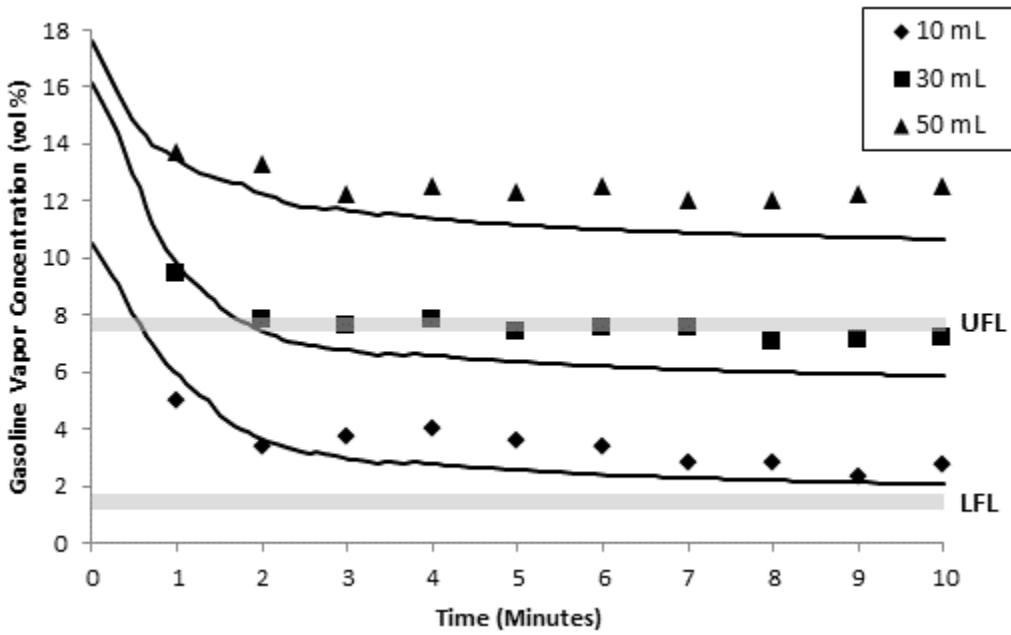


Figure 15. Comparison of experimental data to model predictions for $\alpha = 73^\circ$.

Comparing the data shown from a test angle of 61-degrees (Figure 10) to the data shown for a tilt angle of 73-degrees (Figure 15), the model is less accurate in predicting the flammable vapor zone – particularly at liquid volumes of 30 and 50 mL. At these higher pour angles and larger liquid volumes, the model consistently under-predicts the fuel vapor concentration at longer times. In these cases, the higher evaporation rate may lead to stratification of vapors within the PGC rather than the well-mixed assumption considered in the model.

Overall, the data model successfully captures the experimental for all conditions tested, with a maximum deviation of 2.1 vol% gasoline vapor at the highest pour angle tested, 73 degrees. At these higher pour angles, the assumption of a well-mixed environment in the PGC headspace may need to be modified to account for stratification. In addition, increases in instrumentation sensitivity would likely improve the scatter noted at very low vapor concentrations.

The vapor concentration results obtained from the pour testing experiments are rearranged to show the time duration required for the container headspace to fall within the flammable range. These results are presented in Figure 16 and 17 as a function of liquid volume and container tilt angle, respectively.

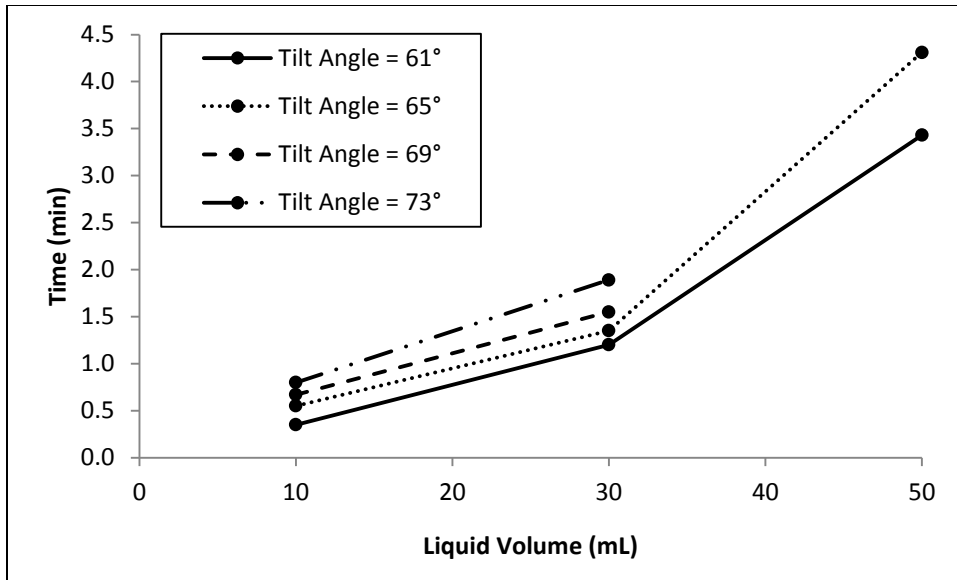


Figure 16. Time required to reach flammable conditions as a function of liquid volume.

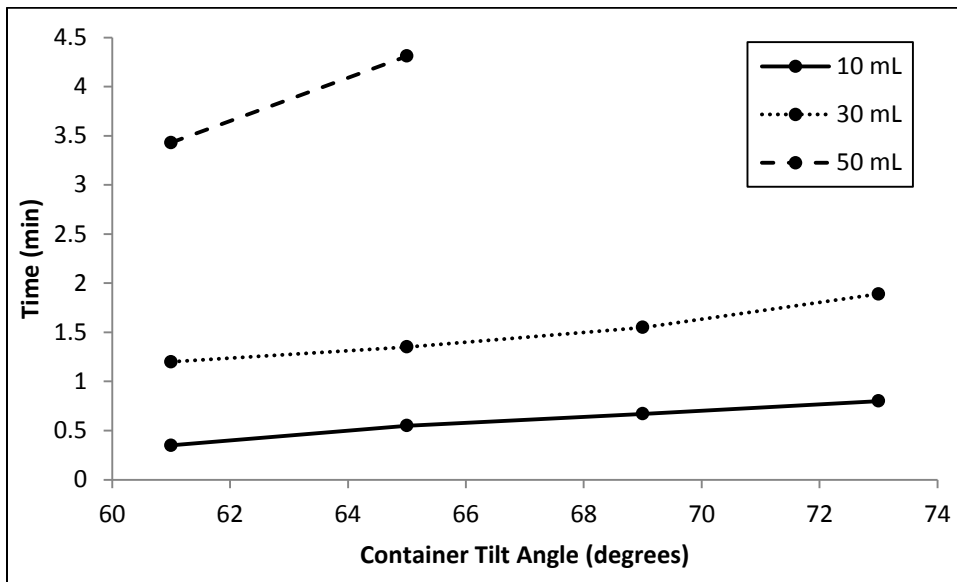


Figure 17. Time required to reach flammable conditions as a function of liquid volume.

Chapter 5

Conclusions

The risk of flame propagation to the inside of a portable gasoline container has been quantified under various scenarios of typical consumer use. A new method is developed to evaluate this hazard based on fuel vapor concentration measurements, which provides a repeatable method for data collection. This method could be applied to test the flammability hazard associated with new portable gasoline container designs without introducing the problems associated with ignition-based testing.

Experimental measurements were conducted in order to identify the controlling parameters for PGC flammability both in storage and pouring scenarios. In a storage environment it is found that both liquid volume and ambient temperature have a significant impact on headspace flammability. In particular, small gasoline volumes and/or low ambient temperatures produce conditions inside the PGC that may allow flame propagation to occur. At -10 °C it is found that liquid volumes of 15 to 30 mL produce a flammable environment inside a static PGC. At 0 °C, 15 mL of liquid fuel is found to produce a flammable environment, while higher liquid volumes resulted in vapor concentrations above the upper flammability limit. At 20 °C, all tested quantities of liquid fuel, from 15 to 1,000 mL produced vapor concentrations above the upper flammability limit.

In the second series of tests, it is found that both the PGC tilt angle and the quantity of liquid fuel effect the vapor concentration along the pour spout length. Using 30 mL of liquid gasoline at 20 °C, it is shown that a flammable concentration of fuel vapor exists at both the pour spout base

and tip for angles of 69 and 71 degrees. The dynamic testing results show that a duration of less than 30 seconds is required for these flammable conditions to exist. These findings suggest that it may be necessary to consider installing flame arresting devices to prevent this type of flame propagation.

Finally, a model to predict the location of the flammable vapor zone within the PGC has been developed that incorporates the primary controlling parameters of temperature, liquid volume, container tilt angle and time. The overall results of the model are promising, and produce good agreement with experimental results particularly at lower tilt angles. This model provides a method to predict the flammability hazard implications of future changes to PGC design or gasoline composition at a far lower cost than laboratory experiments.

References

- [1] M. Danello, *The safety of portable fuel containers (gas cans)*, U.S. Consumer Product Safety Commission Memorandum, 10 Jan 2003.
- [2] L.C. Hasselbring, *Case study: Flame arresters and exploding gasoline containers*, J. Haz. Matls. 130 (2006) 64-68.
- [3] E.A. Tyrrell, *Gasoline and Gasoline Container Fire Incidents*, National Bureau of Standards Technical Note 850, 1975.
- [4] R.A. Harley, S.C. Coulter-Burke, *Relating liquid fuel and headspace vapor composition for California reformulated gasoline samples containing ethanol*, Environ. Sci. Technol. 34 (2000) 4088-4094.
- [5] ASTM International, *ASTM D4814-09b Standard Specification for Automotive Spark-Ignition Engine Fuel*, 2009.
- [6] D.M. Gardiner, M. Bardon, G. Pucher, *An experimental and modeling study of the flammability of fuel tank headspace vapors from high ethanol content fuels*, Nexum Research Corporation, Mallorytown, Canada, 2008.

- [7] J. Arnold, *Studies in Diffusion: III. Unsteady-State Vaporization and Absorption*, Trans. AICHE 30 (1944) 361-378.
- [8] K. Okamoto, N. Watanabe, Y. Hagimoto, K. Miwa and H. Ohtani, *Changes in evaporation rate and vapor pressure of gasoline with progress of evaporation*, Fire Safety Journal 44 (2009) 756-763.
- [9] American Institute of Chemical Engineers, *Guidelines for Chemical Process Quantitative Risk Analysis*, 2000.
- [10] S. Mannan, *Lees' Loss Prevention in the Process Industries*, third ed., Butterworth-Heinemann, 2005.
- [11] J. Hornback, *Organic Chemistry*, second ed., Prentice Hall, Belmont, 2005.
- [12] D. Crowl, J. Louvar, *Chemical Process Safety*, second ed., Prentice Hall, New Jersey, 2002.
- [13] M. Zabetakis, *Flammability Characteristics of Combustible Gases and Vapors*, U.S. Dept. of Interior, Bureau of Mines, Bulletin 627, 1965.
- [14] T.A. Davletshina, N.P. Cheremisinoff, *Fire and Explosion Hazards Handbook of Industrial Chemicals*, William Andrew Publishing/Noyes, Park Ridge, 1998.

Appendix A

Experimental Equipment Photographs



Figure A1. Representative sample of portable gasoline containers used for flammability testing.

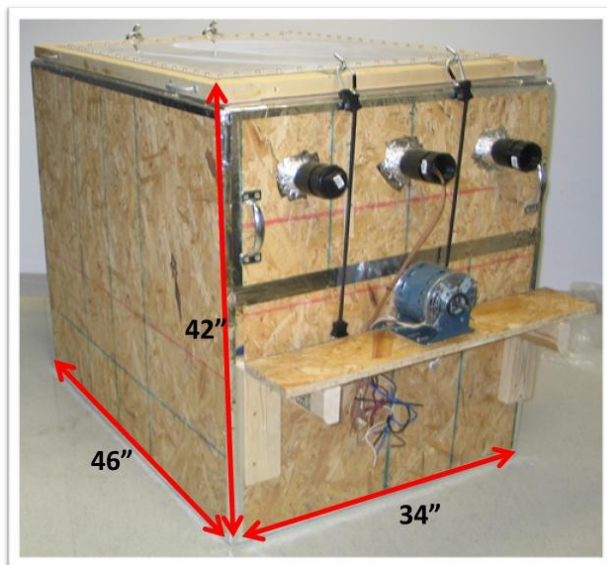


Figure A2. Outside view of environmental chamber used for low temperature testing.

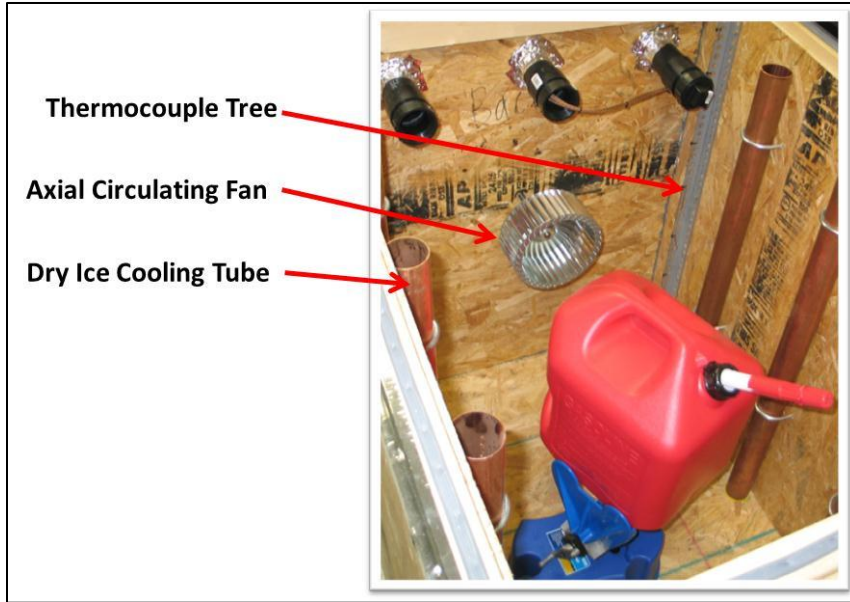


Figure A3. Interior view of environmental chamber.

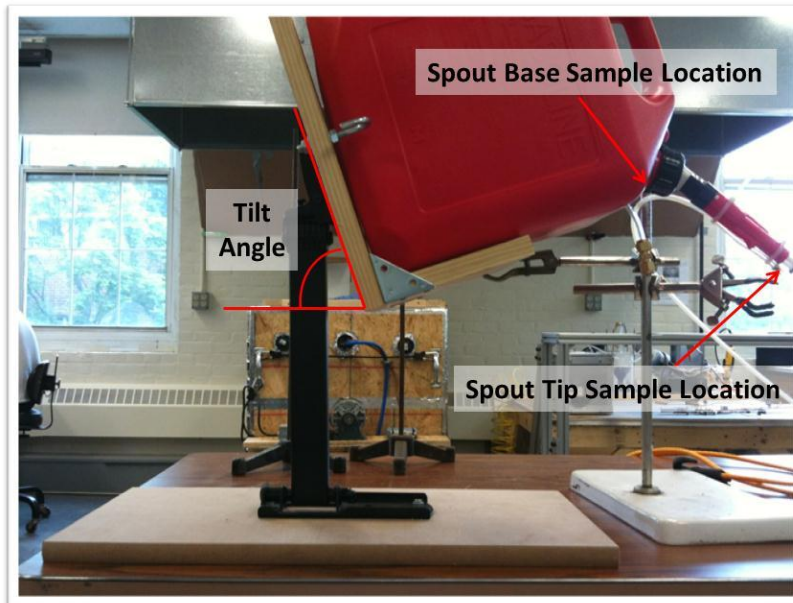


Figure A4. Test apparatus for fuel pouring experiments.



Figure A5. Compressed air apparatus to remove residual fuel vapors.



Figure A6. Environmental chamber with vapor testing instrumentation.

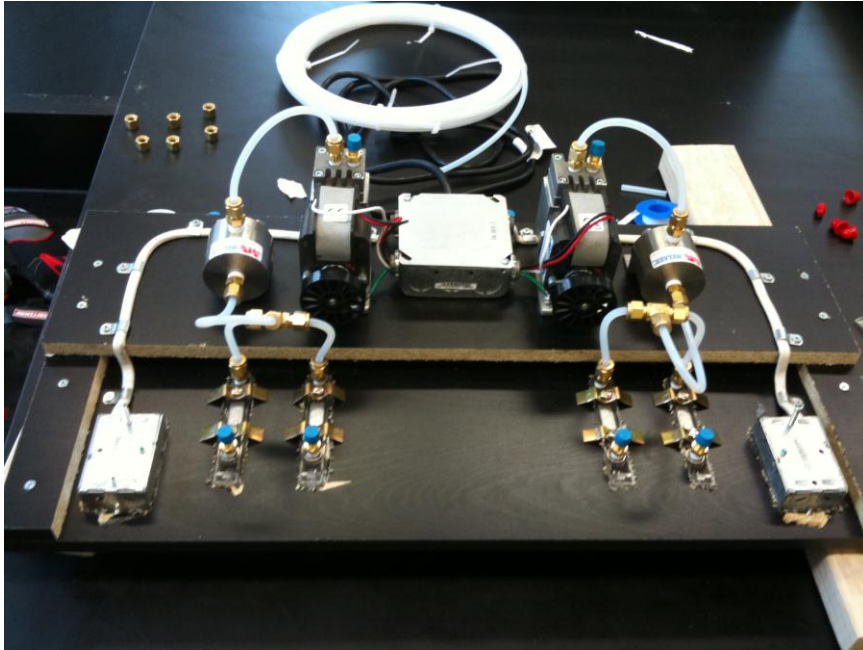


Figure A7. Custom built vapor sampling apparatus including pumps and flow meters.



Figure A8. MSA Altair-5 infrared analyzer used for vapor concentration measurements.



Figure A9. Servomex ServoTough Oxy paramagnetic oxygen analyzer for vapor analysis.



Figure A10. Summa canister used for grab sample acquisition and laboratory analysis.

Appendix B

Computer Code for Mathematical Model

#PGC Model Vapor Concentration Model

#B. Elias, 09/16/2011

#Time Span

t(0) = 0

t(f) = 600

#Overall mass Balance

$d(M_{total}) / dt = \dot{M}_{in} + \dot{M}_{evap} - \dot{M}_{out}$

$\dot{M}_{out} = C * \rho_{pgc} * A * \sqrt{(2 * 9.81 * (\rho_{pgc} - \rho_{inf}) * dz)} / \rho_{pgc}$

$\dot{M}_{in} = \dot{M}_{out} * (\rho_{inf} / \rho_{pgc})$

$\rho_{pgc} = M_{total} / V_{PGC}$

$\dot{M}_{evap} = (S * .306 * \sqrt{0.0851E-4 / (t+1)}) * 2.944$

#Component Mass Balances

$$d(M_G) / d(t) = \dot{m}_{\text{evap}} - y_G \dot{m}_{\text{out}}$$

$$y_G = M_G / M_{\text{total}}$$

$$d(M_{O_2}) / d(t) = 0.23 * \dot{m}_{\text{in}} - y_{O_2} * \dot{m}_{\text{out}}$$

$$y_{O_2} = M_{O_2} / M_{\text{total}}$$

$$d(M_{N_2}) / d(t) = 0.77 * \dot{m}_{\text{in}} - y_{N_2} * \dot{m}_{\text{out}}$$

$$y_{N_2} = M_{N_2} / M_{\text{total}}$$

#Mole Frac Calcs

$$N_G = M_G / 0.072$$

$$N_{O_2} = M_{O_2} / 0.032$$

$$N_{N_2} = M_{N_2} / 0.028$$

$$N_{\text{total}} = N_G + N_{O_2} + N_{N_2}$$

$$X_G = N_G / N_{\text{total}}$$

$$X_{O_2} = N_{O_2} / N_{\text{total}}$$

$$X_{N_2} = N_{N_2} / N_{\text{total}}$$

#Constants

$$R = 8.314$$

$$V_{\text{PGC}} = 0.0189$$

$$T = 298$$

$P_{\text{inf}} = 101325$

$C = 1$

$\rho_{\text{inf}} = 353/T$

$A = 8E-4$

$S = 0.08$

$dZ = 0.3$

#Initial values

$M_{\text{total}}(0) = 0.02766$

$M_G(0) = 0.008961$

$M_{O_2}(0) = 0.004358$

$M_{N_2}(0) = 0.01434$

Appendix C

Photographs of PGC Ignition Testing

Ignition testing was performed on three 5-gallon PGC's produced by different manufacturers. The purpose of the ignition testing was to demonstrate that the conditions identified as hazardous through experimental vapor concentration testing would result in flame propagation. In all three cases, these results were verified as shown in Figure C1 through C3 below.

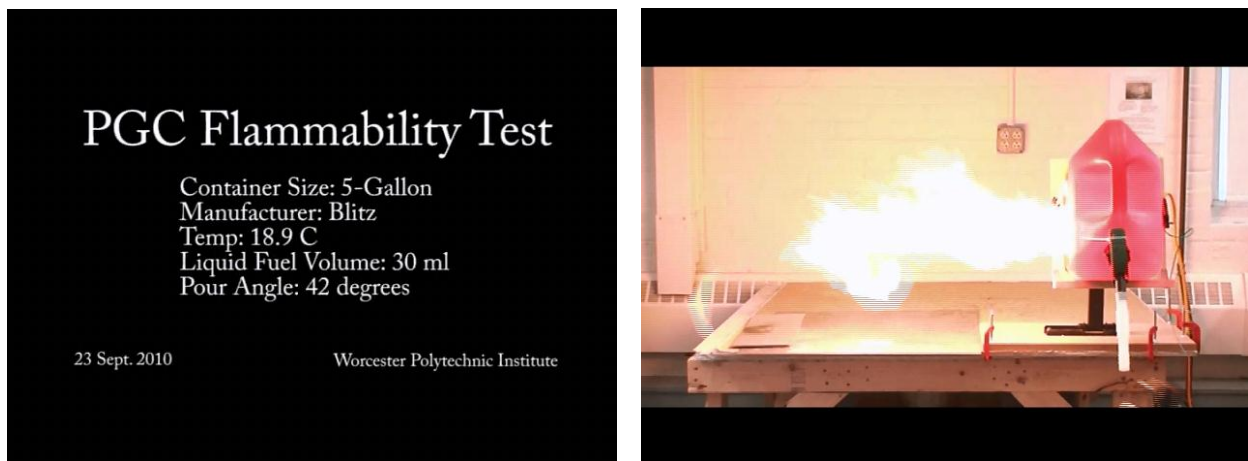


Figure C1. Ignition testing with PGC manufactured by Blitz USA, Incorporated.

PGC Flammability Test

Container Size: 5-Gallon
Manufacturer: Midwest
Temp: 18.9 C
Liquid Fuel Volume: 30 ml
Pour Angle: 42 degrees

23 Sept. 2010 Worcester Polytechnic Institute

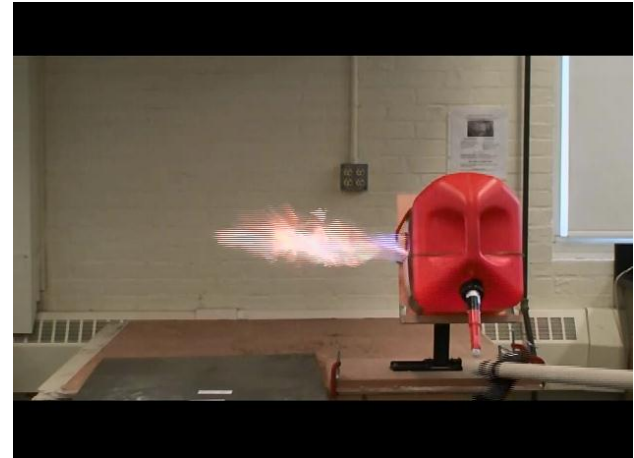


Figure C2. Ignition testing with PGC manufactured by the Midwest Can Company.

PGC Flammability Test

Container Size: 5-Gallon
Manufacturer: Scepter
Temp: 18.5 C
Liquid Fuel Volume: 30 ml
Pour Angle: 42 degrees

28 Sept. 2010 Worcester Polytechnic Institute

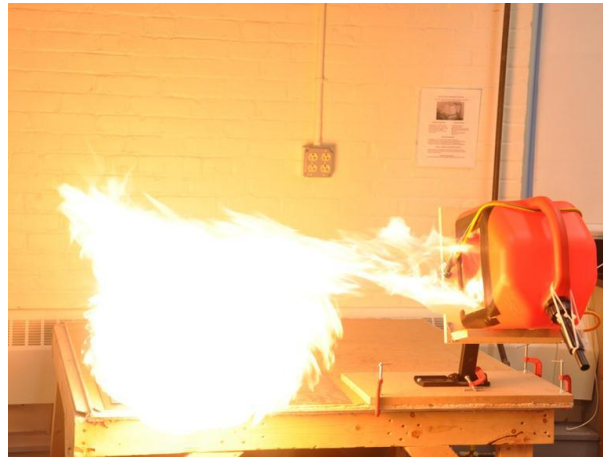


Figure C3. Ignition testing with PGC manufactured by the Scepter Corporation.